PHOTO- AND ELECTROCATALYTIC ACTIVITY OF AN FE(III) COMPLEX CONTAINING A CHELATING ANTIPYRINE LIGAND FOR THE HYDROGEN EVOLUTION REACTION

Amanda C. Mitchell

Advisor: William R. McNamara

Department of Chemistry, College of William & Mary

Abstract

Alternative energy sources need to be explored to prevent worsening consequences of climate change while meeting growing energy demand. The reductive reaction of water splitting through artificial photosynthesis (AP) can produce hydrogen gas that can be used for electricity. When hydrogen gas is burned, water is the only byproduct, making it a clean energy source. Established catalysts for hydrogen evolution integrate rare, expensive metals such as platinum, which would be unsustainable when scaling AP. Our group developed an iron (III) catalyst that is active for electrocatalytic and photocatalytic hydrogen evolution. Electrocatalytic studies demonstrate that the catalyst has modest efficiency and high activity. The catalyst showed stability and yielded high amounts of hydrogen relative to catalyst when tested photocatalytically. The catalyst is also robust as it can photocatalytically produce hydrogen from natural water sources of varying salinity.

Introduction

The industrial revolution triggered the widescale use of fossil fuels for energy, which improved living conditions and increased the human population. Since 1950, energy demand has increased exponentially due to a rapidly growing population and global industrialization.[1] As developing nations expand economically and continue to see their populations quickly increase, it is estimated that global energy demand in 2050 will be double the energy demanded in 2001, jumping from 13.5 terawatts (TW) to 27 TW.[1] It is then estimated that the energy demanded in 2100 will triple to 43 TW compared to 2001.[1] Fossil fuels remain the primary source of energy globally, composing over 75% of global energy composition in 2022 (Figure 1).[2]

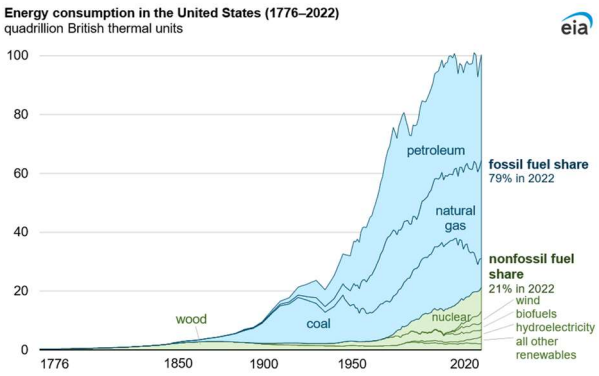

Figure 1. Composition of United States energy consumption from 1776 to 2022.[2]

While there are enough global reservoirs of fossil fuels to sustain increasing energy demand for centuries, fossil fuel consumption has led to a climate crisis that affects environmental and human health through the accumulation of greenhouse gases like carbon dioxide (CO_2).[3] Atmospheric CO_2 has been steadily increasing with a 2.4

ppm average annual increase within the last decade.[3] There is a correlation between increased atmospheric CO_2 and global temperature, with warmer than average global temperatures compared to the 20th century consistently observed since 1980.[4] The increase in global temperature associated with the combustion of fossil fuels has caused a variety of detrimental changes to the environment. These include global sea level rise, more intense heat waves and wildfires, and more extreme weather events like hurricanes.[5] However, the impacts of fossil fuel consumption for energy also threaten human wellbeing, with expected increases in deaths due to disease and extreme heat.[6] The increasing global energy demand and the harm caused to the environment and human health through fossil fuel emissions requires renewable energy alternatives to power the world sustainably into the future.

The two fastest growing renewable energy sources in the United States are wind and solar power.[7] Simultaneously, fossil fuels such as coal are decreasing in their composition of energy generation.[7] While wind and solar energy are clean, renewable, and costs have decreased in recent years, these energy sources are intermittent and require storage for excess energy when electricity cannot be produced.[8,9] Research into battery storage is attempting to keep up with the increase in solar energy capacity, but other energy storage options need to be investigated to meet this growing challenge in renewable energy usage.[10]

Artificial photosynthesis (AP) is a method of using solar energy to generate electricity by splitting water into hydrogen and oxygen gas to meet global energy demand sustainably. Like solar panels, AP can store energy captured from sunlight, but stores energy through chemical bonds instead of batteries. Chemical bonds have a higher energy density than current batteries for photovoltaic cells, and energy can be stored in chemical bonds indefinitely.[11] These advantages of chemical bond storage make AP an exciting option for harnessing solar energy. AP draws inspiration from how photosynthesis occurs naturally in organisms like plants and algae, mimicking the transfer of electrons to split water and produce oxygen and hydrogen. Water splitting consists of two half-reactions: an oxidation of water to oxygen, or the oxygen evolution reaction (OER), and a reduction of protons from water to hydrogen, or the hydrogen evolution reaction (HER) (Scheme 1).[12] Hydrogen can then be ignited to generate energy, with water as a byproduct.[12] Beyond hydrogen generating clean energy on Earth, the production of water as a byproduct of burning hydrogen introduces an opportunity to use sustainable energy on a spacecraft or on a Moon or Mars base while also producing clean drinking water.[13]

$$4H^+ + 4e^- \rightarrow 2H_2$$
$$2H_2O \rightarrow O_2 + 4H^+ + 4e^-$$
$$\overline{2H_2O \rightarrow 2H_2 + O_2}$$

Scheme 1. The reduction and oxidation half-reactions of water splitting.[12]

Both half-reactions of water splitting through AP require a catalyst. Early catalysts developed for the HER used platinum because of its efficiency and its ability to electrochemically reduce protons in aqueous solutions.[14] Platinum catalysts are historically the most effective for performing the HER, but platinum is one of the rarest elements on Earth.[14,15]

The rarity of platinum makes it expensive, deeming platinum catalysts poor candidates to generate hydrogen gas on an industrial scale to meet the growing global energy demand. While heavy metals like platinum and palladium are rare, first-row transition metals like iron and copper are relatively abundant.[15] When trying to develop less expensive HER catalysts that can be scaled, research has investigated using first-row transition metals in these catalysts. Our group focuses on the development of catalysts integrating first row transition metals for hydrogen evolution.

The ability of a catalyst to reduce protons to hydrogen through the HER is assessed using electrochemistry and photochemistry. Electrochemistry, specifically cyclic voltammetry, gives insight into the efficiency and activity of a catalyst. The overpotential of a catalyst is the difference in the equilibrium potential of the reaction of interest, such as the HER, and the potential where the catalyst is active.[16] The overpotential quantifies the efficiency of a catalyst by comparing the extra energy added to the redox potential that the reaction of interest needs to occur.[16] A lower overpotential equates to a more efficient catalyst. The catalytic current enhancement (i_c/i_p) quantifies the activity of a catalyst. The current of the reduction peak of the metal within the catalyst (i_p) with no proton source added is compared to the current of the proton reduction peak (i_c) at the irreversible catalytic wave that appears when a proton source is added to the catalyst.[17] A more active catalyst has a higher catalytic current enhancement. Cyclic voltammograms (CVs) can determine both overpotential and catalytic current enhancement (Figure 2).[17]

Photochemistry is used to determine if a catalyst can undergo the HER using sunlight. Photocatalytic hydrogen generation consists of a photosensitizer, a sacrificial electron donor, and the photocatalyst. The photosensitizer absorbs photons from sunlight, exciting an electron from the photosensitizer. That electron is passed to the catalyst to reduce protons from water and produce hydrogen. To continue this flow of electrons, a sacrificial electron donor gives electrons to the photosensitizer (Figure 3). Turnover numbers (TON), defined as the moles of hydrogen produced per mole of photocatalyst, describes the performance of a photocatalyst.

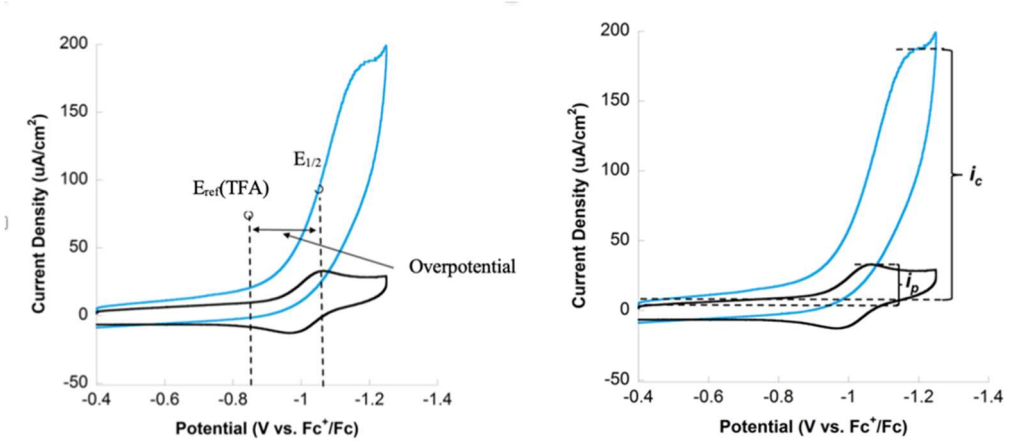

Figure 2. CVs showing (left) the determination of overpotential and (right) the determination of i_c and i_p to determine the catalytic current enhancement.[17]

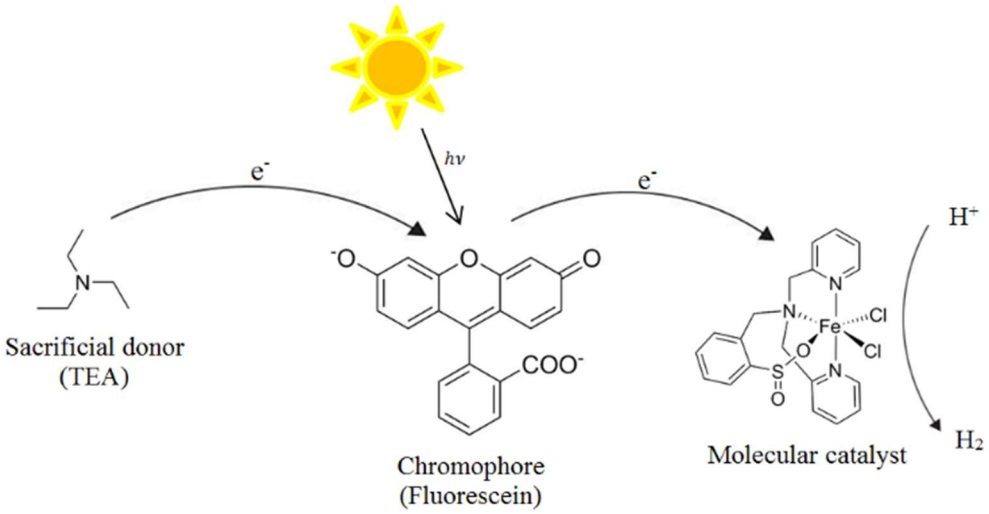

Figure 3. Photocatalytic hydrogen evolution through reductive half-reaction of AP.

This work introduces an iron catalyst with a N,N'- bis(4-antipyrlmethylidene)-ethylenediamine (BAME) ligand that produces hydrogen as both an electrocatalyst and photocatalyst (Figure 4). The electrochemical and photochemical performance of the complex for the HER will be described. We will also discuss the ability of the iron (III) N,N'- bis(4-antipyrlmethylidene)-ethylenediamine (FeBAME) complex to generate hydrogen with natural water sources, such as lake and ocean water, to assess the robustness of the catalyst.

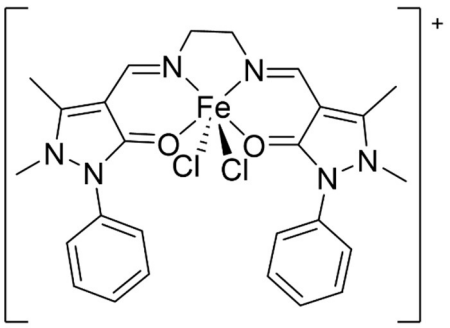

Figure 4. Structure of iron (III) N,N'- bis(4-antipyrlmethylidene)-ethylenediamine (FeBAME) catalyst.

Results and Discussion

Characterization of FeBAME Complex

The crystal structure revealed the iron center of FeBAME has a distorted octahedral geometry, with Fe-N and Fe-O bonds between 2.0 and 2.1 Å. Fe-Cl bonds, ranging from 2.3 to 2.4 Å, were slightly longer than the bonds between iron and BAME. FeBAME has a distorted octahedral geometry as a complex, showing distortions primarily in the O(1)-Fe-O(2) bond, with an angle of 102.9°, and the N(2)-Fe-N(1) bond, with an angle of 76.8°. All other bond angles are less than 10% different than the expected 90° and 180° angles. The bond lengths between O(1)-C(5) and O(2)-C(17) of 1.29 Å and 1.27 Å, respectively, correspond to C double bonded to O in the coordinated ligand. This indicates an L4 coordination geometry of BAME to iron (Figure 5).

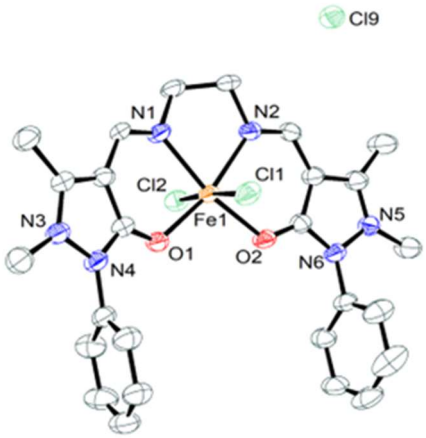

Figure 5. ORTEP diagram of FeBAME with Fe (orange), O (red), N (blue), Cl (green), and C (gray). Hydrogen atoms omitted for clarity and ellipsoids are at a 50% probability level.

Electrocatalytic Hydrogen Evolution

The ability of FeBAME to reduce protons electrochemically was analyzed with a series of cyclic voltammetry studies. CVs of FeBAME alone present a reversible redox couple at -0.43 V vs. Fc^+/Fc, corresponding to the reduction of iron (III) to iron (II). When trifluoroacetic acid (TFA), used as a proton source, is added to FeBAME, the reversible redox couple does not shift, but an irreversible catalytic wave is generated at -1.4 V vs. Fc^+/Fc. The redox couple remaining at -0.43 V vs. Fc^+/Fc means that hydrogen generation occurs through an ECCE or ECEC reaction mechanism. The initial step of the catalysis is a reduction event (E), with a protonation event (C) occurring subsequently, followed by an additional electrochemical step (E). The current density of the irreversible catalytic wave at -1.4 V vs. Fc^+/Fc increases linearly with increasing concentration of TFA, indicating that the reaction is second order with respect to proton concentration (Figure 6).

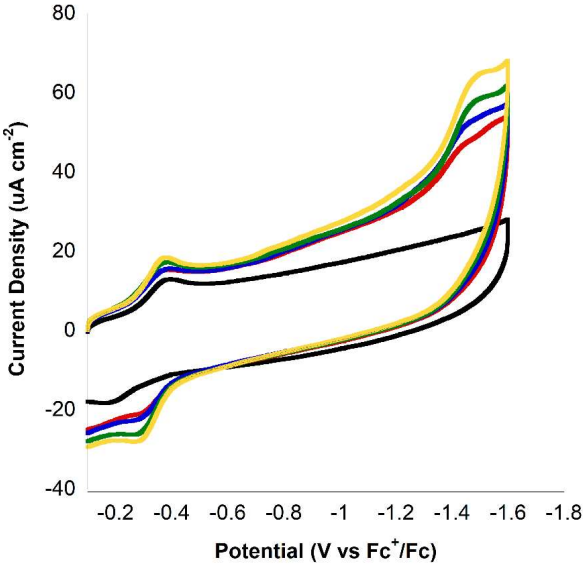

Figure 6. CVs of FeBAME with no acid (black), 0.44 mM (red), 0.66 mM (blue), 0.88 mM (green), and 1.1 mM (yellow) TFA.

The current density also increases linearly with catalyst concentration, demonstrating that the HER is first order with respect to FeBAME (Figure 7). This gives an overall rate expression of rate=$k[FeBAME][H^+]^2$.

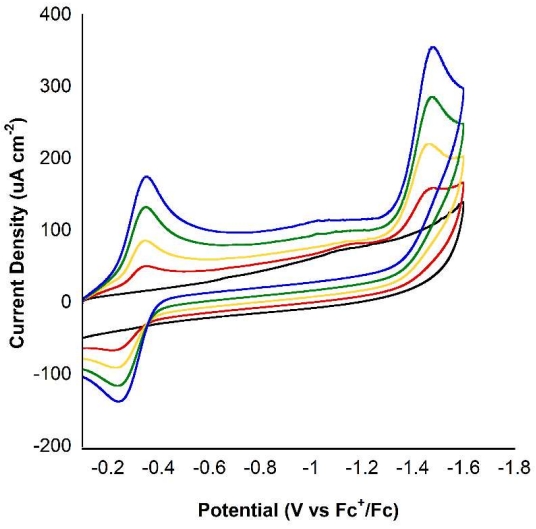

Figure 7. CVs of 22 mM TFA only (black), 97 µM (red), 192 µM (yellow), 286 µM (green), and 377 µM (blue) of FeBAME.

The overpotential and catalytic current enhancement for FeBAME can be calculated using cyclic voltammetry studies to determine the efficiency and activity of FeBAME, respectively. The catalytic current enhancement of FeBAME was calculated as 5.27, demonstrating an active catalyst for the HER. The overpotential of FeBAME in 1.1 mM TFA in acetonitrile was calculated as 700 mV, determined by subtracting the literature value of proton reduction in 1 mM TFA from the half-wave potential of the irreversible catalytic wave representing proton reduction (Equation 1).[18]

$$Overpotential = \left|E_{1/2} - E_{ref}\right|$$

$$= |(-1.4\,V\ vs\ Fc^{+}/Fc) - (-0.71\,V\ vs\ Fc^{+}/Fc)|$$

$$= 700\,mV \qquad (1)$$

Equation 1. Calculation of overpotential of FeBAME in 1.1 mM TFA in acetonitrile.[18]

Photocatalytic Hydrogen Evolution

After it was established that FeBAME can reduce protons electrochemically, the catalyst was analyzed for its photocatalytic ability to perform the HER. System optimization studies determined fluorescein as the ideal photosensitizer and triethylamine (TEA) as the optimal sacrificial electron donor for photocatalytic hydrogen evolution with FeBAME. When irradiated with visible light with a wavelength of 520 nm, hydrogen evolution was observed consistently over 36 hours, reaching TONs greater than 1700 (Figure 8). This demonstrates the stability of FeBAME in aqueous solution while undergoing irradiation and the longevity of hydrogen evolution using this catalyst.

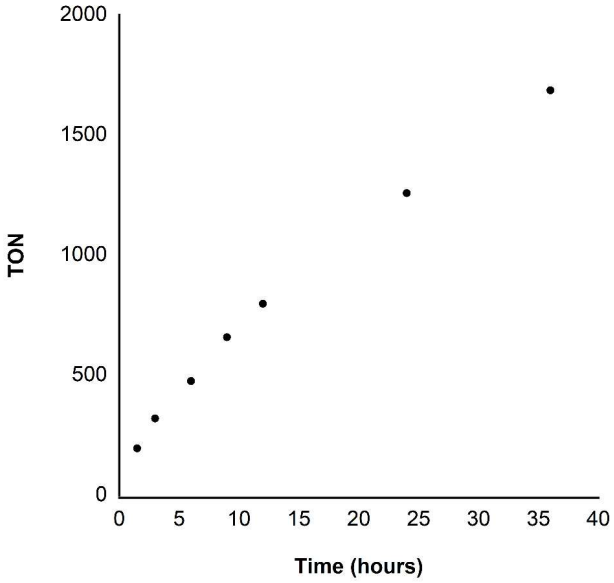

Figure 8. TONs over 36 hours for 7.5 μM FeBAME with 1.8 mM FI and 5% TEA in 1:1 water:ethanol.

When addressing how photocatalytic hydrogen generation will be implemented on a larger scale, or be used for applications like deep space exploration, it is important to discuss the salinity of the water source that will be split to make hydrogen. As fresh and salt water are more abundant globally than deionized water, we wanted to test the ability of FeBAME in generating hydrogen with impure, natural water sources. Fresh lake water, brackish bay water, and saltwater from the ocean were tested, replacing deionized water as the proton source in the photocatalytic system. The studies conducted with lake, bay, and ocean water generated hydrogen for over 30 hours. Maximum TONs over 800 were reached for lake water, 260 for bay water, and 330 for ocean water (Figure 9). These results correspond to other catalysts in our group tested with lake water, where lake water generated TONs that were about half of the TONs generated when using deionized water.[19]

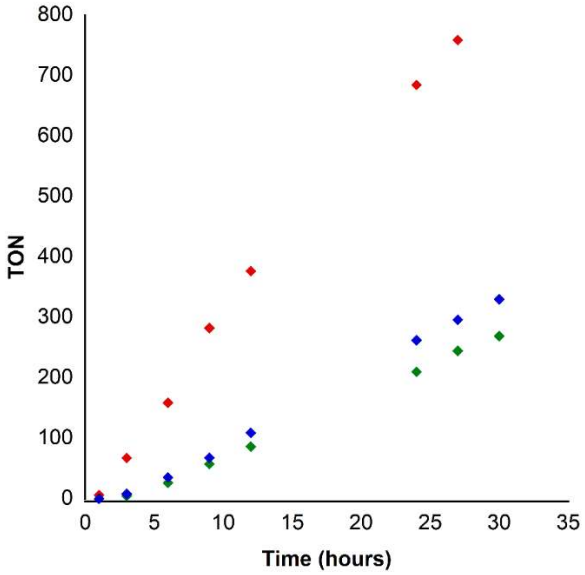

Figure 9. TONs over 30 hours when integrating lake (red), bay (green), and ocean (blue) water instead of deionized water for photocatalytic hydrogen evolution with FeBAME.

Conclusion

An iron catalyst with the BAME ligand was synthesized, characterized, and successfully reduced protons to produce hydrogen under electrocatalytic and photocatalytic conditions. The crystal structure of the catalyst demonstrates a distorted octahedral geometry and suggests L4 binding of BAME to iron. FeBAME was shown to be more efficient and active than previous iron catalysts developed in our group, with an overpotential of 700 mV and a catalytic current enhancement of 5.27. Photocatalytic generation of hydrogen using FeBAME was optimized in a system with fluorescein as the photosensitizer and TEA as the sacrificial electron donor, reaching TONs greater than 1700 over 36 hours. The catalyst is also robust enough to produce hydrogen in natural water sources with varying salinity. FeBAME is an exciting catalyst for performing the HER, with future research in our group focusing on complexing BAME with other first-row transition metals and synthesizing derivatives of the ligand. The success of this catalyst demonstrates the potential of using the HER to generate hydrogen for clean energy to lessen the use of fossil fuels on Earth and to produce reliable energy for space travel.

Acknowledgements

ACM thanks the Office of Graduate Studies and Research, the Chemistry Department of the College of William & Mary, and the Virginia Space Grant Consortium for funding. ACM also thanks Jess Cropley and Nicole Fritsch for their contributions to this project. WRM thanks the National Science Foundation and the Camille and Henry Dreyfus foundation for funding.

References

1. Hoffert, M. I.; Caldeira, K.; Jain, A. K.; Haites, E. F.; Harvey, L. D. D.; Potter, S. D.; Schlesinger, M. E.; Schneider, S. H.; Watts, R. G.; Wigley, T. M. L.; Wuebbles, D. J. Energy Implications of Future Stabilization of Atmospheric CO_2 Content. *Nature* **1998**, 395 (6705), 881–884. https://doi.org/10.1038/27638.
2. Nonfossil fuel energy sources accounted for 21% of U.S. energy consumption in 2022 - U.S. Energy Information Administration (EIA). https://www.eia.gov/todayinenergy/detail.php?id=56980 (accessed 2024-03-25).
3. Lewis, N. S.; Nocera, D. G. Powering the Planet: Chemical Challenges in Solar Energy Utilization. *Proc Natl Acad Sci U S A* **2006**, 103 (43), 15729–15735.

https://doi.org/10.1073/pnas.0603395103.
4. If carbon dioxide hits a new high every year, why isn't every year hotter than the last? | NOAA Climate.gov. http://www.climate.gov/news-features/climate-qa/if-carbon-dioxide-hits-new-high-every-year-why-isn%E2%80%99t-every-year-hotter-last (accessed 2024-03-26).
5. Seneviratne, S. I.; Zhang, X.; Adnan, M.; et al.; Cambridge University Press: Cambridge, United Kingdom and New York, NY, USA, 2021, 1513–1766. https://doi.org/10.1017/9781009157896.001.
6. Climate change. https://www.who.int/news-room/fact-sheets/detail/climate-change-and-health (accessed 2024-03-26).
7. Renewable generation surpassed coal and nuclear in the U.S. electric power sector in 2022. https://www.eia.gov/todayinenergy/detail.php?id=55960 (accessed 2024-03-26).
8. Advantages and Challenges of Wind Energy. Energy.gov. https://www.energy.gov/eere/wind/advantages-and-challenges-wind-energy (accessed 2024-03-26).
9. Solar. IEA. https://www.iea.org/energy-system/renewables/solar-pv (accessed 2024-03-26).
10. Solar Photovoltaic Cell Basics. Energy.gov. https://www.energy.gov/eere/solar/solar-photovoltaic-cell-basics (accessed 2024-03-25).
11. Revankar, S. T. Chapter Six - Chemical Energy Storage. In Storage and Hybridization of Nuclear Energy; Bindra, H., Revankar, S., Eds.; *Academic Press* **2019**, 177–227. https://doi.org/10.1016/B978-0-12-813975-2.00006-5.
12. Eckenhoff, W. T.; McNamara, W. R.; Du, P.; Eisenberg, R. Cobalt Complexes as Artificial Hydrogenases for the Reductive Side of Water Splitting. *Biochimica et Biophysica Acta (BBA) - Bioenergetics* **2013**, 1827 (8), 958–973. https://doi.org/10.1016/j.bbabio.2013.05.003.
13. NASA's Lunar Trailblazer Gets Final Payload for Moon Water Hunt - NASA. https://www.nasa.gov/missions/small-satellite-missions/lunar-trailblazer/nasas-lunar-trailblazer-gets-final-payload-for-moon-water-hunt/ (accessed 2024-03-26).
14. Gray, H. B. Powering the Planet with Solar Fuel. *Nature Chem* **2009**, 1 (1), 7–7. https://doi.org/10.1038/nchem.141.
15. Rare Earth Elements—Critical Resources for High Technology | USGS Fact Sheet 087-02. https://pubs.usgs.gov/fs/2002/fs087-02/ (accessed 2024-03-26).
16. Appel, A. M.; Helm, M. L. Determining the Overpotential for a Molecular Electrocatalyst. *ACS Catal.* **2014**, 4 (2), 630–633. https://doi.org/10.1021/cs401013v.
17. Connor, G. P.; Mayer, K. J.; Tribble, C. S.; McNamara, W. R. Hydrogen Evolution Catalyzed by an Iron Polypyridyl Complex in Aqueous Solutions. *Inorg. Chem.* **2014**, 53 (11), 5408–5410. https://doi.org/10.1021/ic500069c.
18. Hoffert, W. A.; Roberts, J. A. S.; Bullock, R. M.; Helm, M. L.

Production of H2 at Fast Rates Using a Nickel Electrocatalyst in Water–Acetonitrile Solutions. *Chem. Commun.* **2013**, 49 (71), 7767–7769. https://doi.org/10.1039/C3CC43203C.

19. Hartley, C. L.; DiRisio, R. J.; Screen, M. E.; Mayer, K. J.; McNamara, W. R. Iron Polypyridyl Complexes for Photocatalytic Hydrogen Generation. *Inorg. Chem.* **2016**, 55 (17), 8865–8870. https://doi.org/10.1021/acs.inorgchem.6b01413.